McSharry, J. J., & Wagner, R. R. (1971) *J. Virol. 7*, 59-70.
Miller, D. K., Feuer, B. I., Vanderoef, R., & Lenard, J. (1980) *J. Cell Biol. 84*, 421-429.
Mudd, J. A. (1974) *Virology 62*, 573-577.
Petri, W. A., Jr., & Wagner, R. R. (1979) *J. Biol. Chem. 254*, 4313-4316.
Petri, W. A., Jr., & Wagner, R. R. (1980) *Virology 107*, 543-547.
Petri, W. A., Jr., Estep, T. N., Pal, R., Thompson, T. E., Biltonen, R. L., & Wagner, R. R. (1980) *Biochemistry 19*, 3088-3091.
Rose, J. K., Welch, W. J., Sefton, B. M., Esch, F. S., & Ling, N. C. (1980) *Proc. Natl. Acad. Sci. U.S.A. 77*, 3884-3888.
Schloemer, R. H., & Wagner, R. R. (1975) *J. Virol. 16*, 237-249.
Shinitzky, M., & Barenholz, Y. (1974) *J. Biol. Chem. 249*, 2652-2657.
Shinitzky, M., & Barenholz, Y. (1978) *Biochim. Biophys. Acta 515*, 367-394.
Sklar, L. A., Miljanich, G. P., & Dratz, E. A. (1979) *Biochemistry 18*, 1707-1716.
Suurkuusk, J., Lentz, B. R., Barenholz, Y., Biltonen, R. L., & Thompson, T. E. (1976) *Biochemistry 15*, 1393-1401.
Tilley, L., Thulborn, K. R., & Sawyer, W. H. (1979) *J. Biol. Chem., 254*, 2592-2594.
Toneguzzo, F., & Ghosh, H. P. (1978) *Proc. Natl. Acad. Sci. U.S.A. 75*, 715-719.
Wagner, R. R. (1975) in *Comprehensive Virology* (Fraenkel-Conrat, H., & Wagner, R. R., Eds.) Vol. 4, pp 1-93, Plenum Press, New York.

Fluorescence Lifetime and Time-Resolved Polarization Anisotropy Studies of Acyl Chain Order and Dynamics in Lipid Bilayers†

Paul K. Wolber‡ and Bruce S. Hudson*,§

ABSTRACT: The time-resolved fluorescence intensity and anisotropy decays of *cis*- and *trans*-parinaric acids and phosphatidylcholines labeled with *trans*-parinaric acid have been characterized in bilayers formed by several phosphatidylcholines and by dipalmitoylphosphatidylcholine–cholesterol mixtures, at several temperatures. Both a conventional free-running nitrogen flashlamp and the novel synchrotron source at the Stanford Linear Accelerator Center (SLAC) were used as excitation sources for a modified single photon counting fluorescence lifetime apparatus. The measured emission decay kinetics of both isomers of parinaric acid were biexponential in all but one of the lipid systems examined. The fluorescence anisotropy of parinaric acid was large and constant in gel phase lipids, but showed a very rapid (~2 GHz) decay of large amplitude in fluid lipids. In all lipid systems studied, the fluorescence anisotropy decayed to a nonzero asymptote, in striking contrast to the behavior observed in viscous solvent solutions. The asymptotic anisotropy was used to calculate an "order parameter" of the emission transition dipole. The value of the order parameter is quite close to that obtained by deuterium NMR. Cholesterol increased the order parameter measured in fluid dipalmitoylphosphatidylcholine but did not substantially affect the rate of angular relaxation. Experiments conducted with *trans*-parinaroylphosphatidylcholines yielded results virtually identical with those obtained with *trans*-parinaric acid.

Investigations of the dynamic and order properties of the angular degrees of freedom of acyl chains in phospholipid bilayers are important for several reasons. The phospholipid bilayer is the foundation of biological membranes, and the phospholipid acyl chains form the environment of many functionally important membrane proteins. Phospholipid bilayers are also intrinsically interesting structures. They can be modeled theoretically only after extending or rethinking techniques for dealing with isotropic three-dimensional systems. The existence of phospholipid phase transitions, involving collective disordering of the acyl chains, expands the scope and content of such modeling by introducing phase equilibria and large changes in order and dynamics. Finally, most of our knowledge of the effect of other membrane lipids (e.g., cholesterol) and membrane proteins on the structure of lipid bilayers comes from studies of their effect on the acyl chain dynamics and order.

The properties of acyl chains in bilayers have been investigated with a broad spectrum of techniques, including X-ray scattering (Rand et al., 1975; Janiak et al., 1976; Brady & Fein, 1977), ^{2}H NMR (Seelig & Seelig, 1974a,b; Brown & Seelig, 1979; Stockton & Smith, 1976; Oldfield et al., 1978; Davis, 1979; Brown, 1979), ^{1}H NMR (Hemminga & Berendson, 1972; Seiter & Chan, 1973), nitroxide ESR (Hubbell & McConnell, 1971; Jost et al., 1971), polarized, time-resolved fluorometry (Chen et al., 1977; Kawato et al., 1977), and phase fluorimetry (Lakowicz et al., 1979). The overall trends seen by magnetic resonance techniques have been recently reviewed by Bocian & Chan (1978), and the results of ESR and deuterium NMR have been compared by Gaffney & McConnell (1974).

Polarized, time-resolved fluorometric techniques have several advantages over other methods. First, both dynamic and order information can be extracted from the decay data in a straightforward way. Since experiments are performed in the time rather than frequency domain, the dynamic information

† From the Department of Chemistry, Stanford University, Stanford, California 94305, and the Department of Chemistry and Institute of Molecular Biology, University of Oregon, Eugene, Oregon 97403. *Received September 18, 1980.* This work was supported by grants from the National Institutes of Health (GM21149 and GM26536).

‡ Present address: Cardiovascular Research Institute, University of California, San Francisco, CA 94143.
§ Present address: Department of Chemistry, University of Oregon, Eugene, OR 97403. National Institutes of Health Research Career Development Awardee (GM00476).

0006-2960/81/0420-2800$01.25/0

which is obtained from the short time behavior is clearly separated from the order measurements which come from the long time data. Finally, fluorescence-based methods are quite sensitive and can be applied to small volumes of dilute samples. These advantages must usually be weighed against several disadvantages. Fluorescent probes are often bulky, potentially perturbing molecules. The location and orientation of a fluorescent probe in the bilayer are often unknown. In addition, time-resolved, polarized fluorescence experiments are usually time consuming and difficult to perform with sufficient temporal resolution.

The present work utilizes a unique set of well-characterized, fluorescent fatty acid probes, *trans*-parinaric acid (*all-trans*-9,11,13,15-octadecatetraenoic acid) and *cis*-parinaric acid (cis,trans,trans,cis isomer of *trans*-parinaric acid) (Sklar et al., 1975, 1977a,b). These probes closely resemble the acyl chains of phospholipids, are located at a known depth and with a known orientation in the bilayer, and can be incorporated as one of the acyl chains of a phosphatidylcholine molecule. They also have fluorescent lifetimes which are well suited to studies of bilayer dynamics.

The difficulties inherent in performing polarized, time-resolved fluorescence studies have been partially circumvented in this work by using the synchrotron radiation available at the Stanford Linear Accelerator Center (SLAC) as an excitation source (Munro et al., 1979). This tunable, rapidly repeating source of very narrow pulses is a nearly ideal excitation source for time-resolved fluorometry. As shall be seen, the quality of the excitation source is not critical for order parameter measurements but is critical for dynamics measurements.

Experimental Procedures

Materials. Dipalmitoylphosphatidylcholine (DPPC)[1] (Sigma or Calbiochem) was used as purchased, unless explicitly stated otherwise. Dielaidoylphosphatidylcholine (DEPC) was synthesized and purified by the methods of Gupta et al. (1977) under nitrogen in the absence of strong light. Cholesterol (Aldrich) was recrystallized 3 times from methanol. Cholesterol (crystals) and DEPC (chloroform solution) were stored under nitrogen. All lipids were stored at −20 °C and were pure as judged by thin-layer chromatography (Analabs silica gel G).

The cis and trans isomers of parinaric acid were prepared by published methods (Sklar et al., 1977b, 1980). Parinaric acid stock solutions were stored in ethanol containing BHT (1–10 mol % parinaric acid) under argon in black-taped containers at −20 °C. The phospholipid probes 1-myristoyl-2-*trans*-parinaroyl-*sn*-glycero-3-phosphocholine (MtPnPC) and 1-stearoyl-2-*trans*-parinaroyl-*sn*-glycero-3-phosphocholine (StPnPC) were prepared by published methods (Morgan et al., 1980; Tsai et al., 1980) and stored under the same conditions as parinaric acid.

Cyclohexanol (Baker reagent grade) was purified by treatment with activated charcoal, followed by distillation under nitrogen. All buffers were prepared from reagent grade materials, vacuum freeze–thaw degassed, and stored under argon at 4 °C. Hepes, EDTA, and L-histidine were purchased from Sigma. Two buffer systems were used, Hepes–histidine (10 mM Hepes, 10 mM L-histidine, 1 mM EDTA, and 100 mM NaCl) and phosphate (100 mM potassium phosphate), both in the pH range 7.0–7.5.

Phospholipid Samples. Ethanol injection vesicles were typically prepared from 30 mg/mL ethanolic solutions of phosphatidylcholines by the methods of Kremer et al. (1977). Residual ethanol was allowed to leak from the vesicles by holding them at the lipid-transition temperature for ~15 min and then annealing 10–15 °C above the transition temperature for ~10 min. This treatment sharpened the phase transitions of injection vesicles (as observed by *trans*-parinaric acid fluorescence) to the 1–2 °C width observed for multilamellar vesicles. This treatment did not cause fusion of the vesicles, as judged by the ability of the samples to pass through a 400-nm Millipore filter and the 80–100-nm diameter range observed in negative stained electron micrographs of the vesicles. In a few cases, residual ethanol was removed by passage of the vesicles through a Sephadex G-100 column or by dialysis.

Parinaroyl phospholipids and cholesterol were dispersed into injection vesicles by adding the extra lipids to the ethanol stock solution at the desired mole fraction. Care was taken to protect these samples from oxygen and light. Dispersions containing cholesterol were injected into buffer at least 20 °C above the phosphatidylcholine phase transition.

Multilamellar vesicles (Bangham, 1972) were prepared by drying chloroform solutions of phosphatidylcholines first under a stream of nitrogen and then under vacuum for at least 1 h, adding buffer, heating at least 10 °C above the phase transition, and vortexing 2 times for 30 s, with reheating between vortexing. The methods and precautions used for multilamellar vesicles containing parinaroylphosphatidylcholines and/or cholesterol were the same as those used when injection vesicles were prepared.

Lipid dispersions were labeled with free parinaric acid by injection of a 2 mM ethanolic aliquot of parinaric acid solution into the dispersion, at a temperature above the lipid phase transition.

Fluorescence Experiments. Static fluorometry was performed with a Spex Fluorolog fluorometer, modified to automatically alternately sample polarized and depolarized fluorescence as a function of temperature. Lipid phase transition temperatures were measured by observing the discontinuous decrease in parinaric acid fluorescence polarization and quantum yield at the transition (Sklar et al., 1977b).

Time-resolved, polarized fluorometry was performed with either a flashlamp-excited, Ortec time-resolved fluorometer or the apparatus in place at SLAC (Munro et al., 1979). The flashlamp apparatus was basically of the type described by Isenberg (1975). A slow, steady stream of atmospheric pressure nitrogen flowed through the free-running lamp, which was biased at ~7 kV. For elimination of rf pickup, the flashlamp and its power supply were completely isolated electrically from the rest of the apparatus. A portion of the lamp pulse, coupled via a Lucite light pipe to a 1P21 photomultiplier, was used to generate the time to pulse height converter start signal (Leskovar et al., 1976). The lamp flash was passed through a J-Y H-10 monochrometer and a Glan–Thompson polarizer. The emission was viewed by an RCA 8850 photomultiplier through a Polaroid polarizer, followed by a combination of long-pass and interference filters (Oriel

[1] Abbreviations used: BHT, butylated hydroxytoluene (2,6-di-*tert*-butyl-*p*-cresol); cPnA, *cis*-parinaric acid (9-*cis*,11-*trans*,13-*trans*,15-*cis*-octadecatetraenoic acid); DEPC, 1,2-dielaidoyl-*sn*-glycero-3-phosphocholine; DMPC, 1,2-dimyristoyl-*sn*-glycero-3-phosphocholine; DPPC, 1,2-dipalmitoyl-*sn*-glycero-3-phosphocholine; DSPC, 1,2-distearoyl-*sn*-glycero-3-phosphocholine; EDTA, ethylenediaminetetraacetic acid; Hepes, *N*-(2-hydroxyethyl)piperazine-*N*′-2-ethanesulfonic acid; MtPnPC, 1-myristoyl-2-*trans*-parinaroyl-*sn*-glycero-3-phosphocholine; SLAC, Stanford Linear Accelerator Center; StPnPC, 1-stearoyl-2-*trans*-parinaroyl-*sn*-glycero-3-phosphocholine; tPnA, *trans*-parinaric acid (9-*trans*,11-*trans*,13-*trans*,15-*trans*-octadecatetraenoic acid).

and Melles–Griot, respectively). Scattered light was determined by using an unlabeled blank sample. Temperature control was achieved by means of water-jacketed, 5-mm path-length quartz cuvettes connected to a thermostated recirculating water bath. The sample temperature was monitored by a thermocouple directly inserted in the sample cuvette.

The δ function excitation response of the system was approximated by a sum of exponential decays and was determined by fitting the observed response, $F(t)$, measured at the fluorophore emission maximum, to the form

$$F(t) = \sum_{i=1}^{N} A_i \int_0^{t-Q} E(t-Q-t')e^{-t'/\tau_i}\,dt' \qquad (1)$$

by means of a nonlinear least-squares routine (Shrager, 1970; Grinvald & Steinberg, 1974). In eq 1, N is the number of decay components, the A_i and τ_i are preexponential weighting factors and lifetimes, respectively, $E(t)$ is the excitation pulse shape (measured at the excitation wavelength), and Q is the time shift introduced by the different ejection energies of excitation and emission photoelectrons (Gafni et al., 1975). The factor Q was determined for a given series of experiments by measuring the fluorescence of a 10^{-6} M ethanolic solution of 9-cyanoanthracene (Aldrich) under the same conditions used for parinaric acid. The decay was fit to a single exponential, with Q as a fit parameter. The determined value of Q ($\sim$0.3 ns for excitation at 316 nm and emission at 420 nm) was then used as a fixed parameter for fits performed on parinaric acid emission data.

The quality of numerical fits was monitored by plotting the modified residuals (residuals divided by the square root of the number of counts) and the Poisson weighted autocorrelation function of the residuals. Both functions should look like random noise for a good fit (Grinvald & Steinberg, 1974). In all cases, Poisson weighted fits to two decades of decay were performed. Extensive confidence tests have been performed on the apparatus, computer software, and the procedures used to subtract scatter and determine Q. The test results along with a detailed description of the apparatus and counting sequences are described elsewhere (Wolber, 1980).

The measured emission transients parallel [$I_{VV}(t)$] and perpendicular [$I_{VH}(t)$] to the vertical excitation polarization were used to form the difference [$F_D(t)$] and total [$F_T(t)$] decay functions. The emission optics did not introduce any

$$F_D(t) = I_{VV}(t) - I_{VH}(t) \qquad (2a)$$

$$F_T(t) = I_{VV}(t) + 2I_{VH}(t) \qquad (2b)$$

polarization bias, as judged by the equality of the vertically and horizontally polarized transients excited with horizontally polarized light.

The difference and total decays were deconvoluted by means of eq 1 in the following fashion. First, $F_T(t)$ was fit with a sum of two exponentials. Then, $F_D(t)$ was fit with a sum of three exponentials, with one of the lifetimes fixed at a value equal to τ_1, the longest lifetime obtained in the fit to $F_T(t)$. This fitting form assumes that the time-resolved emission anisotropy, $r(t)$, decays to a nonzero asymptote (Wolber, 1980). There are five parameters to be adjusted in the fit to $F_D(t)$.

The fit approximation to the deconvoluted time-resolved anisotropy was then formed in a striaghtforward manner:

$$r(t) = \frac{[A_\infty^{(D)} e^{-t/\tau_1^{(T)}} + \sum_{i=1}^{2} A_i^{(D)} e^{-t/\tau_i^{(D)}}]}{\sum_{j=1}^{2} A_j^{(T)} e^{-t/\tau_j^{(T)}}} \qquad (3)$$

where $A_i^{(D)}[\tau_i^{(D)}]$ and $A_j^{(T)}[\tau_j^{(T)}]$ are the preexponential factors (lifetimes) determined by fits to $F_D(t)$ and $F_T(t)$, respectively, and $A_\infty^{(D)}$ is the fifth parameter in the fit to $F_D(t)$.

The order and kinetic properties were quantified as the order parameter, S, and the ensemble average inverse rotational correlation time, $\langle\phi^{-1}\rangle$, respectively (Kinosita et al., 1977):

$$S \equiv \left\langle \frac{1}{2}(3\cos^2\theta - 1) \right\rangle = (r_\infty/r_0)^{1/2} \qquad (4a)$$

$$\langle\phi^{-1}\rangle \equiv 6\langle D_w\rangle = -\lim_{t\to 0} \frac{d}{dt}\,[r(t)/r_0] \qquad (4b)$$

In eq 4a, θ is the angle between the fluorophore emission transition dipole and the local bilayer normal, r_∞ is the asymptotic anisotropy, and r_0 is the zero-time (or limiting) anisotropy. In eq 4b, D_w is the "wobbling diffusion coefficient". The brackets $\langle\,\rangle$ denote ensemble averaging.

Two forms of r_∞ were calculated. The first, $r_\infty^{(fit)}$, derived from the fit results, is given by

$$r_\infty^{(fit)} = A_\infty^{(D)}/A_1^{(T)} \qquad (5)$$

The second, $r_\infty^{(tail)}$, was calculated by averaging five consecutive values of the anisotropy calculated directly from $I_{VV}(t)$ and $I_{VH}(t)$, after two decades of decay.

The quantities $A_j^{(D)}$ and $A_j^{(T)}$ are arbitrarily scaled. The corresponding scaled quantities χ_j and d_j are defined by

$$\chi_j \equiv A_j^{(T)}/\sum_j A_j^{(T)} \qquad (6a)$$

$$d_j \equiv A_j^{(D)}/\sum_j A_j^{(T)} \qquad (6b)$$

Note that the χ_j sum to unity, while the d_j sum to $r(0)$, the fit approximation to r_0.

Results

Solvent Studies. The difference and total decays of *cis*- and *trans*-parinaric acids were measured in cyclohexanol and cyclohexanol/butanol mixtures by using synchrotron excitation. The decays for cyclohexanol measured at SLAC are shown in Figure 1. The values of the fit zero time anisotropy, $r(0)$, calculated from the fits to the decays were 0.38 (*trans*-parinaric acid) and 0.37 (*cis*-parinaric acid), in good agreement with the r_0 values of 0.39 and 0.38 (*trans*- and *cis*-parinaric acids, respectively) found by Kaplan (S. Kaplan, personal communication) for the static fluorescence anisotropy from a propylene glycol glass. The total decay kinetics were well fit by single exponentials.

Fluid solution studies with flashlamp excitation have, by contrast, typically extrapolated to values of $r(0)$ between 0.23 and 0.28 (Wolber, 1980). For determination of the source of this discrepancy, the fluorescence anisotropy decay of fluorescein in 95% glycerol/5% aqueous NaOH (corrected to 10 °C) was measured with flashlamp excitation. Under these conditions, fluorescein is known to be completely immobilized, with $r(t) = r_0 = {}^2/_5$ (Chen & Bowman, 1965). The measured corrected value of r_0 for fluorescein in the flashlamp apparatus was 0.35, indicating some depolarization within the apparatus. The rest of the discrepancy between the observed and expected values of r_0 was probably caused by the severity of the deconvolution problem for the flashlamp data in the solvents studied. The fluorescence lifetimes and rotational relaxation times were all typically shorter than the full width at half-maximum of the excitation pulse. This source of error in $r(0)$ is indicated by the observation that $r(0)$ decreased as the viscosity of the solvent decreased. In alcohol solvents, both isomers of parinaric acid always exhibited single-exponential total decays. (Alcohol solvents were used to discourage dimer

Table I: Total Fluorescence Decays in Gel Phase Lipids at 23 °C

lipid	probe	[lipid] (mg/mL)	probe/lipid	χ_1	$\tau_1^{(T)}$ (ns)	χ_2	$\tau_2^{(T)}$ (ns)
DPPC[a]	tPnA	0.2	1:400	0.74	50.3	0.26	14.7
DPPC[a]	tPnA	0.1	1:200	0.73	50.2	0.27	14.1
DPPC[a]	tPnA	0.05	1:100	0.74	50.1	0.26	14.2
DPPC[b]	StPnPC	0.1	1:200	0.77	46.0	0.23	9.2
DSPC[b]	StPnPC	0.1	1:200	0.76	61.0	0.24	12.7
DPPC[a]	MtPnPC	0.3	1:400	0.69	50.5	0.31	6.9

[a] Ethanol injection vesicles, Hepes–histidine buffer. [b] Multilamellar vesicles, phosphate buffer. All data were obtained with flashlamp excitation.

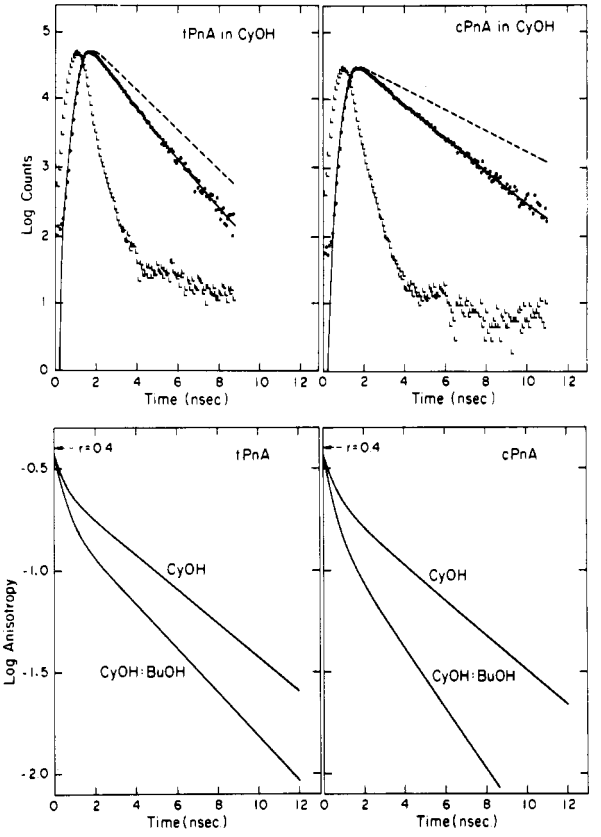

FIGURE 1: Synchrotron-excited parinaric acid fluorescence decays in cyclohexanol and anisotropy decays in cyclohexanol and cyclohexanol/butanol, 5:1. The temperature was 23 °C. In the upper panels, the difference decay data have been scaled to match the peak heights of the total decay data. The symbol "L" denotes the excitation pulse. The lifetimes obtained for *trans*- (*cis*-) parinaric acid were $\tau^{(T)}$ = 1.4 (2.7) ns. The weighting parameters and lifetimes obtained from the difference decays were d_1 = 0.12 (0.14), d_2 = 0.26 (0.23), $\tau_1^{(D)}$ = 0.34 (0.46) ns, and $\tau_2^{(D)}$ = 1.1 (1.8) ns. The difference decay calculated with these parameters is shown as a solid line through the difference data. The total decay is shown as a dashed line without data. The anisotropy decay curves calculated from these fits are shown in the lower panels. These anisotropy decays can be described in terms of two rotational correlation times. For cyclohexanol, the values of τ_R are 0.45 and 5.2 ns for *trans*-PnA and 0.56 and 5.0 ns for *cis*-PnA. For cyclohexanol/butanol the values are 0.53 and 4.0 ns for tPnA and 0.52 and 2.9 ns for cPnA.

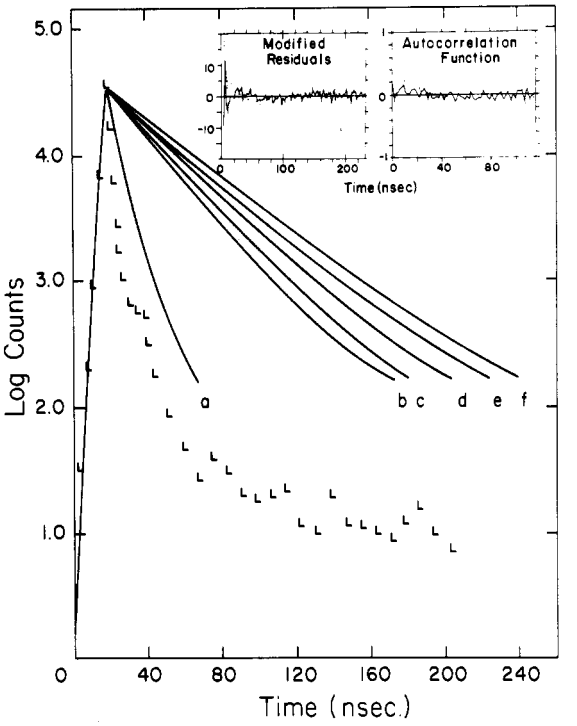

FIGURE 2: Flashlamp-excited fluorescence decays of *trans*-parinaric acid in DPPC ethanol injection vesicles. Sample temperatures (°C) were (a) 43.0, (b) 39.9, (c) 38.0, (d) 35.0, (e) 32.0, and (f) 29.9. All buffers were Hepes–histidine, pH 7.0. The inset at the top right shows the modified residual and residual autocorrelation functions calculated for one- (···) and two- (—) exponential fits to the decay obtained at 29.9 °C (curve f). The autocorrelation function shows that a single-exponential fit gives rise to deviations which are systematic.

and inverse micelle formation.)

These solvent results influence the interpretation of the bilayer results subsequently reported to two ways. First, a value of r_0 = 0.35 has been used for all parinaric acid data measured with the flashlamp apparatus, as opposed to a value of $r_0 = {}^2/_5$ for data taken at SLAC. Second, the extrapolated value of r_0 has been used as a confidence test of the fits to the early time difference decays.

Intensity Decays in Lipid Vesicles. The fluorescence intensity decays of parinaric acid and its phosphatidylcholine derivatives were biexponential in all gel phase lipid systems examined. A summary of several key *trans*-parinaric acid experiments is shown in Table I. Plots of the modified residual and autocorrelation functions derived from one- and two-exponential fits are shown in Figure 2, alone with decay curves obtained at several temperatures.

Arrhenius plots of both lifetimes for both *cis*- and *trans*-parinaric acids in DPPC were linear (Wolber, 1980) and yielded a scattered range of activation energies averaging to 7.7 ± 3.5 kcal mol^{-1} for the temperature-dependent deexcitation process. The lifetimes did not sense the pretransition in DPPC. These findings are in agreement with previously reported results for parinaric acid in DPPC (Sklar et al., 1977b).

The intrinsic or radiative lifetime of both isomers of parinaric acid is reasonably independent of environment (Sklar et al., 1977a; Andrews & Hudson, 1978). This implies that the normalized preexponential factors (χ_i) from fits to parinaric acid total fluorescence decays are the mole fractions of parinaric acid exhibiting the lifetime τ_i. The mole fractions of *cis*- and *trans*-parinaric acids exhibiting long lifetimes in gel phase DPPC are plotted as a function of temperature in Figure 3. The fraction of parinaric acid exhibiting a long

Table II: Total Fluorescence Decays in Fluid Phase Lipids

lipid	probe	[lipid] (mg/mL)	probe/lipid	temp (°C)	χ_1	$\tau_1^{(T)}$ (ns)	χ_2	$\tau_2^{(T)}$ (ns)	$\bar{\tau}$
DPPC[a]	MtPnPC	0.30	1:400	47.5	0.51	4.49	0.49	1.85	3.20
DPPC[a]	MtPnPC	0.20	1:200	53.0	0.20	4.38	0.80	2.02	2.49
DPPC[a]	tPnA	0.25	1:160	53.0	0.30	3.63	0.70	1.87	2.40
DPPC[b]	tPnA	0.25	1:160	53.0	0.11	4.49	0.89	2.27	2.51
DPPC[c]	tPnA	0.10	1:100	59.0	0.32	2.53	0.68	1.35	1.73
DEPC[b]	tPnA	0.10	1:150	23.0	0.50	6.82	0.50	3.13	4.98
DEPC[b]	tPnA	0.10	1:150	35.0	0.17	7.08	0.83	3.03	3.72
DEPC[b]	tPnA	0.10	1:150	46.0	0.04	6.57	0.96	2.25	2.42
DEPC[b]	cPnA	0.10	1:150	23.0	0.56	7.10	0.44	3.10	5.34
DEPC[b]	cPnA	0.10	1:150	35.0	0.17	7.08	0.83	3.03	3.72
DEPC[b]	cPnA	0.10	1:150	46.0	0.09	6.57	0.91	2.79	3.13

[a] Ethanol injection vesicles, phosphate buffer, flashlamp excitation. [b] Liposomes, phosphate buffer, flashlamp excitation. [c] Liposomes, phosphate buffer, synchrotron excitation.

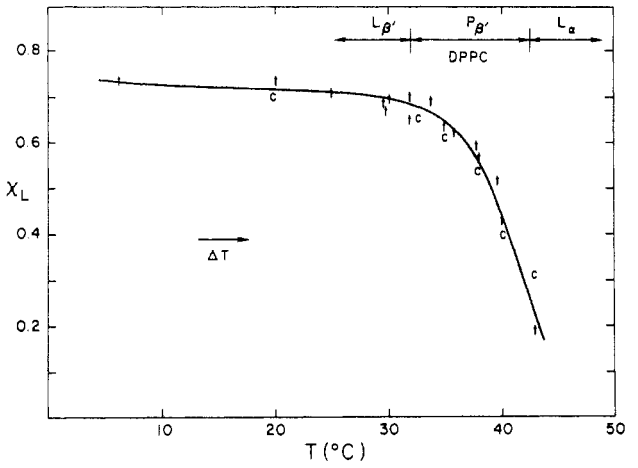

FIGURE 3: Mole fraction of parinaric acid exhibiting a long lifetime (χ_L) in DPPC ethanol injection vesicles, as a function of temperature. Points are plotted for both *trans*- (t) and *cis*- (c) parinaric acids. The gel ($L_{\beta'}$), pretransitional ($P_{\beta'}$), and fluid (L_α) phase regions for DPPC are marked in the upper right corner. The symbol ΔT denotes the direction in which the temperature was changed. The buffer was Hepes–histidine, pH 7.0; labeling was 1 parinaric acid/200 lipids.

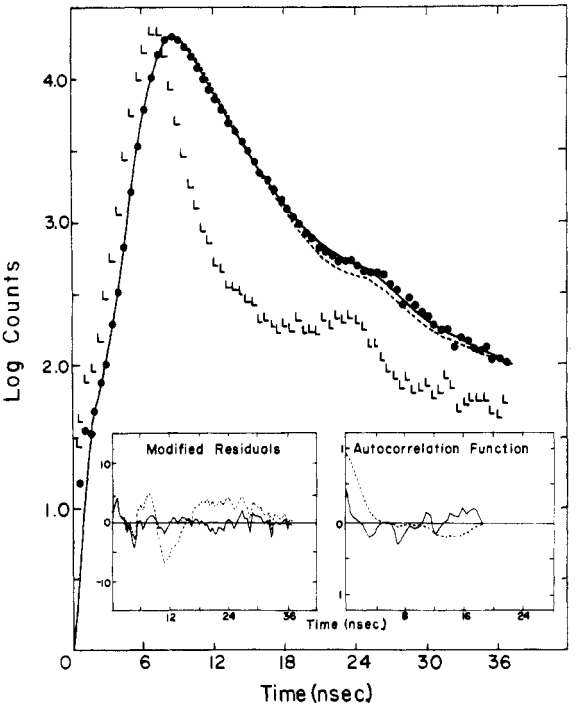

FIGURE 4: Flashlamp-excited fluorescence decay of *trans*-parinaric acid in DPPC injection vesicles at 53 °C. The best single- (---) and double- (—) exponential fits are shown. Solid circles denote the data points for the fluorescence; L's denote the lamp excitation pulse shape. The lifetime obtained with the single-exponential fit was 2.6 ns. The double-exponential fit gave lifetimes of 1.9 and 3.6 ns with relative weights of 0.7 and 0.3. (The mean lifetime calculated from this fit, $\chi_1\tau_1 + \chi_2\tau_2$, is 2.4 ns.) The insets show the modified residuals and autocorrelation functions with the same line convention. The double-exponential fit clearly reduces the systematic error.

lifetime clearly exhibits premelting behavior. The effect does not depend on the isomer used.

In nearly all of the fluid lipids examined, the fluorescence decays of both isomers of parinaric acid were inadequately fit by single-exponential test functions and well fit by double-exponential test functions. The key data are summarized in Table II. A typical decay and fit, along with plots of statistical test functions, are shown in Figure 4.

For investigation of the nature of the lifetime heterogeneity observed in fluid lipids, several experiments were conducted with multilamellar vesicles made from DEPC. The low (~13 °C) transition temperature of DEPC allowed the investigation of the fluorescence decay of parinaric acid in a fluid lipid under conditions where the average fluorescence lifetime was relatively long so that the deconvolution problem was minimized. The results of several experiments at different temperatues are given in Table II. The data clearly demonstrate that, at least in DEPC, the parinaric acid lifetime homogeneity increases as the difference between the experimental and transition temperatures increases.

The effects of cholesterol on gel- and fluid-phase lifetimes in DPPC are shown in Table III. In the gel phase of DPPC, the chief effect of cholesterol was to decrease the mole fraction of parinaric acid exhibiting a long lifetime. In the fluid phase, the effects seen were more complicated, consisting of modulations of both preexponential factors and lifetimes. Clearly, however, the overall effect of cholesterol on the fluid phase of DPPC was to increase the average lifetime and therefore the quantum yield.

Anisotropy Decays in Lipid Vesicles. A typical parinaric acid total and difference fluorescence decay pair obtained at SLAC is shown in Figure 5. Plots of the fit exponential approximations to $r(t)$ (eq 3) for *trans*-parinaric acid in DPPC and two DPPC–cholesterol mixtures are shown in Figures 6 and 7. A more complete summary of the data obtained from both flashlamp and synchrotron excited experiments is presented in Table IV.

In the total–difference decay pair shown in Figure 5 (and all other such pairs obtained at SLAC), the two decay functions, when plotted logarithmically, are parallel at long times, in striking contrast to the solvent behavior shown in Figure

Table III: Total Fluorescence Decays in DPPC–Cholesterol Mixtures

temp (°C)	x_c[a]	probe	x_1	τ_1(T) (ns)	x_2	τ_2(T) (ns)
20	0.0[b]	tPnA	0.86	49.1	0.14	10.7
	0.1[b]	tPnA	0.77	49.2	0.23	9.7
	0.2[b]	tPnA	0.72	48.1	0.28	9.3
	0.3[b]	tPnA	0.65	44.3	0.35	13.5
	0.0[b]	cPnA	0.75	26.3	0.25	8.6
	0.1[b]	cPnA	0.71	26.0	0.29	6.3
	0.2[b]	cPnA	0.65	26.2	0.35	8.9
	0.3[b]	cPnA	0.63	24.3	0.37	7.4
53	0.0[c]	MtPnPC	0.20	4.4	0.80	2.0
	0.1[c]	MtPnPC	0.40	4.7	0.60	2.1
	0.2[c]	MtPnPC	0.52	5.6	0.48	2.4
	0.3[c]	MtPnPC	0.62	6.7	0.38	2.7
59	0.0[d]	tPnA	0.32	2.5	0.68	1.3
	0.1[d]	tPnA	0.59	2.6	0.41	0.8
	0.2[d]	tPnA	0.55	3.8	0.44	1.5

[a] Mole percent cholesterol. [b] Injection vesicles, flashlamp excitation, Hepes–histidine, 0.27 mM lipid, 1 probe/135 lipids. [c] Injection vesicles, flashlamp excitation, phosphate buffer, 0.40 mM lipid, 1 probe/400 lipids. [d] Multilamellar vesicles, SLAC, phosphate buffer, 0.15 mM lipid, 1 probe/100 lipids.

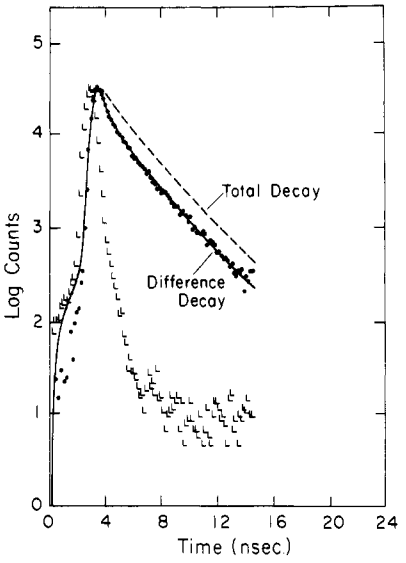

FIGURE 5: Synchrotron radiation excited fluorescence decays of *trans*-parinaric acid in DPPC/10% cholesterol multilamellar vesicles at 59 °C. The scaling and symbols are the same as for Figure 1. The fit parameters are $\chi_1 = 0.59$, $\tau_1 = 2.6$ ns, $\chi_2 = 0.41$, $\tau_2 = 0.8$ ns, $d_1 = 0.22$, $\tau_1^{(D)} = 0.23$ ns, $d_2 = 0.033$, $\tau_2^{(D)} = 1.1$ ns, and $d_3 = 0.044$. These yield values of $r(0) = 0.30$ and $r_\infty^{(fit)} = 0.074$. (See Tables III and IV.) The anisotropy decay calculated with these parameters is one of the curves of Figure 7.

1. This behavior is not so obvious in data obtained with flashlamp excitation, although Table IV shows that the fits to the observed behavior as well as direct calculation from the decay tail indicate decay to a constant, nonzero value of r. One of the chief advantages of synchrotron excitation is that the important physical effect, i.e., a constant anisotropy at long times, is clearly revealed by the raw data.

It is obvious from the extrapolated values of $r(0)$ in Table IV that the flashlamp system, under the conditions employed, was not capable of resolving the early anisotropy decay in either fluid or pretransitional gel lipids, although the flashlamp system did measure an acceptably high value of $r(0)$ in gel DPPC below the pretransition. It should be noted that the one experiment in which the flashlamp system did measure a high value of $r(0)$ (MtPnPC, 47.5 °C) was the result of

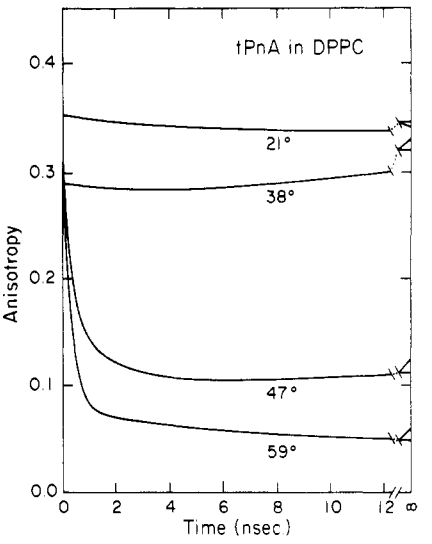

FIGURE 6: Anisotropy decay curves for parinaroyl chains in DPPC at various temperatures. The 21, 38, and 47 °C curves refer to experiments performed with myristoyl-*trans*-parinaroyl-phosphatidylcholine in DPPC ethanol injection vesicles (0.2 mg/mL) and flashlamp excitation. The probe to lipid ratios were 1:400 for the 21 and 38 °C curves and 1:200 for the 47 °C curve. The 59 °C curve refers to *trans*-parinaric acid in DPPC multilamellar vesicles at a probe to lipid ratio of 1:200. Synchrotron radiation was used for this experiment. For each curve, there are two lines at the right-hand margin representing $r_\infty^{(fit)}$ (horizontal line) and $r_\infty^{(tail)}$ (slanting line). (See footnote 2.)

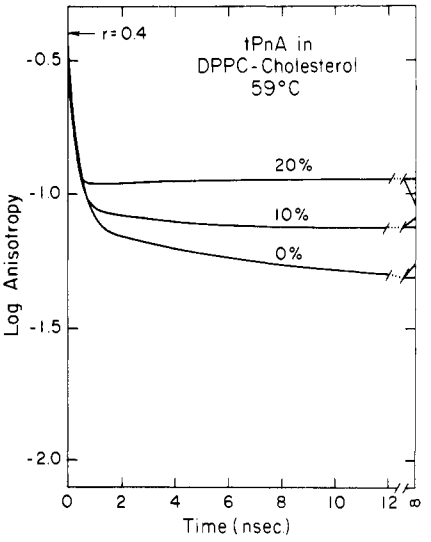

FIGURE 7: Anistotropy decay curves for *trans*-parinaric acid in DPPC–cholesterol mixtures at 59 °C. The samples are multilamellar vesicles in phosphate buffer, 0.15 mM lipid, and a probe to lipid ratio of 1:100. The parameters used to construct these curves are given in Tables III and IV.

meticulous fine tuning of the flashlamp (full width at half-maximum of the excitation pulse was <2 ns). In our hands, the Ortec flashlamp has maintained such good pulse quality for only brief periods of time.

Discussion

The total fluorescence decay of both *cis*- and *trans*-parinaric acids in cyclohexanol solution can be accurately represented by a single exponential (Figure 1). This is an important observation because it demonstrates that the double-exponential behavior observed in bilayer experiments is not inherent to these chromophore preparations. It also serves as a test of the data collection and analysis procedures under fairly stringent short lifetime, low quantum yield conditions. The

Table IV: Difference Fluorescence Decays in DPPC/Cholesterol Bilayers

χ_c[a]	temp (°C)	probe	d_1	τ_1(D) (ns)	d_2	τ_2(D) (ns)	d_3	$r(0)$	$\langle\phi^{-1}\rangle$ (GHz)	r_∞(fit)	S_{fit}	r_∞(tail)	S_{tail}
0.0[b]	21.0	MtPnPC	0.11	5.8			0.24	0.35	e	0.35	0.93	0.34	0.92
0.0[b]	38.0	MtPnPC	0.12	3.9			0.17	0.29	e	0.32	0.89	0.33	0.91
0.0[b]	47.5	MtPnPC	0.17	0.27	0.11	1.4	0.056	0.34	e	0.080	0.45	0.12	0.55
0.0[b]	47.5	tPnA	0.18	0.61	0.055	2.0	0.010	0.25	e	0.097	0.49	0.12	0.54
0.0[b]	53.0	MtPnPC	0.20	0.63	0.057	2.4	0.011	0.27	e	0.055	0.37	0.064	0.40
0.0[c]	59.0	tPnA	0.24	0.27	0.059	1.4	0.016	0.32	1.9	0.048	0.35	0.055	0.37
0.1[b]	53.0	MtPnPC	0.18	0.62	0.057	3.1	0.038	0.27	e	0.095	0.52	0.12	0.59
0.1[c]	59.0	tPnA	0.22	0.23	0.033	1.1	0.044	0.30	2.0	0.074	0.43	0.098	0.49
0.2[b]	53.0	MtPnPC	0.14	1.0	0.043	4.2	0.069	0.25	e	0.13	0.61	0.15	0.65
0.2[c]	59.0	tPnA	0.37	0.13	0.046	1.5	0.070	0.48[d]	6.7[d]	0.11	0.52	0.093	0.48
0.3[b]	53.0	MtPnPC	0.086	1.4			0.14	0.23	e	0.23	0.81	0.18	0.72

[a] Mole percent cholesterol. [b] Flashlamp excitation. [c] Synchrotron excitation. [d] Known to be in error. [e] Values for the apparent $\langle\phi^{-1}\rangle$ were obtained for these flashlamp experiments. For the solid phase (21 and 38 °C), the values were 0.01 GHz, indicating very slow motion. The 47.5 °C MtPnPC value was 1.5 GHz. Note that $r(0)$ is quite high for this experiment and that the value is slightly less than the 59.0 °C synchrotron value. The 47.5 °C tPnA and 53.0 °C MtPnPC values were 0.58 and 0.53 GHz. Note the low values of $r(0)$ in these cases. The 53.0 °C values with the cholesterol/DPPC mixtures are also low, as are the values of $r(0)$.

fluorescence lifetimes obtained from the total decay measurements were 1.4 ns for *trans*-parinaric acid and 2.7 ns for *cis*-parinaric acid.

The time-dependent anisotropy $r(t)$ for solutions also serves as a valuable test of our methods. The values of $r(0)$ of 0.38 and 0.37 are very close to the theoretical value of r_0 of $^2/_5$. This demonstrates that the instrument used is capable of resolving very rapid anisotropy decays. The decay of the anisotropy toward a zero value at long times is, of course, the behavior expected for isotropic solution. The more viscous solvent cyclohexanol (η = 0.68 g cm^{-1} s^{-1}) shows a less rapid decay than the less viscous mixture of cyclohexanol/butanol (5:1, η = 0.54 g cm^{-1} s^{-1}). The overall behavior of $r(t)$ in solution is consistent with the coupling of the rigid body motion of the polyene chromophore with internal isomerization of the upper methylene segment (Evans, 1979; Knauss & Evans; Evans & Knauss, 1980) and the quantitative determination of Bauer et al. (1975).

Another important consideration in the interpretation of the polarization anisotropy of parinaric acid is the degree to which the polyene chromophore (carbon atoms 9–16 and the hydrogens bonded to these carbons) can be considered to be a rigid unit. The barrier for conversion from the s-trans to the s-cis isomer of butadiene is known from Raman spectroscopy to be about 7.2 kcal mol^{-1} (Carreira, 1975). Corresponding theoretical estimates are 10 kcal mol^{-1} (Warshel & Karplus, 1972; Lasaga, 1976). For reference, the trans–gauche barrier for methylene chains is only 3 kcal mol^{-1}. Thus, the rate of interconversion between conformers involving bond rotations within the polyene chromophore will be much too slow to influence fluorescence measurements. Also, the free energy difference between the s-cis and s-trans conformers of about 2.5 kcal mol^{-1} for butadiene corresponds to roughly a 1% population of the s-cis state for each polyene single bond at room temperature. Thus, we assume that the polyene chromophore is both rigid and fully extended.

The fluorescence decays observed for the parinaroyl chromophore in gel phase lipids clearly consists of two (or more) exponential components. The observed lifetimes and component amplitudes are quantitatively independent of the fluorescent probe concentration in the range 1:100 to 1:400 (probe/lipid) (Table I). The same behavior is observed for parinaric acid and parinaroyl-labeled phospholipids (Table I), and the amplitude of the long-lifetime component is independent of the parinaric acid isomer used (Figure 3). Furthermore, the preparative method used to make the bilayers (ethanol injection or vortexing) has no significant effect. Vesicles formed from DMPC by a detergent-dilution method exhibited long- and short-lifetime components at 10 °C similar to those observed for DPPC and DSPC (Wolber, 1980). The smooth temperature dependence shown in Figure 3 demonstrates that the amplitude of the long-lifetime component is a highly reproducible quantity. Temperature cycling and annealing had no effect on the amplitude of the exponential components.

Taken as a whole, these experiments indicate that the parinaroyl chromophore is sensitive to some kind of disorder which is inherent to gel-phase lipids. Several other techniques give evidence for the presence of residual disorder in both the L_β' and P_β' gel phases (freeze–fracture electron microscopy: Luna & McConnell, 1977; Watts et al., 1978; Krbecek et al., 1979; Raman spectroscopy: Gaber & Peticolas, 1977; Yellin & Levin, 1977a,b; deuterium NMR: Paddy et al., 1980). Low-temperature deuterium NMR studies indicate a very wide range of order parameters. The Raman studies demonstrate the presence of some gauche bonds in the acyl chains. The continuous variation in the amplitude of the short-lifetime component with temperature in the P_β' phase (Figure 3) parallels the observed Raman spectral parameter changes and the variation in the lateral diffusion coefficient (Smith & McConnell, 1978). Also, the values of the lifetimes observed for the short-lifetime component are close to those obtained by extrapolation of the high-temperature fluid phase behavior into the gel phase temperature region (Sklar et al., 1977b).

All of these observations are consistent with a picture of the gel phase in which some of the phospholipid acyl chains have a conformation and possibly dynamic behavior which is, in some respects, similar to that found in the high-temperature fluid L_α phase. The behavior of the anisotropy for gel phase DPPC is of interest in this respect (Figure 6). The L_β' curve (21 °C) and especially the P_β' (38 °C) gel phase curves fall below their asymptotic values and then increase. The only reasonable explanation of this behavior is that a relatively long lifetime component has a higher limiting anisotropy than a short lifetime component. This means that, to the extent that there are only two lifetime components, the species with the short lifetimes (τ_2) has a lower anisotropy and a lower order parameter (see below) than the long-lived species. This further indicates that the short-lived species has properties similar to that of a fluid-phase bilayer.

The effect of cholesterol on the total fluorescence decay of parinaric acid in bilayers at low temperature is also of interest.

The major effect (Table III, 21 °C data) is that an increase in cholesterol content increases the fraction of the short lifetime ("fluid") component without appreciably changing the lifetimes of the two apparent components.

The fluorescence decay of parinaric acid in fluid bilayers can be described with reasonable accuracy as a single-exponential decay (Figure 4, dashed line). Similar fits have been reported for the fluorescence of diphenylhexatriene in lipid bilayers (Kawato et al., 1977). However, a double exponential gives a considerably improved fit to the data. This is particularly important, in a fractional sense, in the long time region. This has also been noted for diphenylhexatriene (Chen et al., 1977). When a double-exponential fit is performed, the average lifetime ($\chi_1\tau_1 + \chi_2\tau_2$) is very close to the value obtained from the single-exponential fit. Our major reason for using the double-exponential fit is that, since it gives a more accurate description of the total decay curve, it will result in a more accurate determination of the anisotropy decay.

It is important to point out that a chromophore is not expected to have a single fluorescence lifetime except under special circumstances. What is expected is a distribution of lifetimes corresponding to the variety of environments and conformational states available to the chromophore. The exceptions where single-exponential behavior will be a good approximation are when there is only one environmental or conformational state, where there is interconversion between all such states on a short time scale compared to the excited-state lifetime, or where the chromophore is not very sensitive to its environmental or conformational state.

The experiments shown in Table II, particularly the DEPC results, show that at higher temperatures the heterogeneity of the decay is decreased. This may indicate a more rapid interconversion between states with different lifetimes or a decreased population of some states with a long lifetime. The individual weighting factors and lifetimes obtained from the double-exponential fit probably do not have much physical significance for several reasons. The first is that there is probably a distribution of lifetimes as discussed above. The second is that, since the lifetimes only differ by about a factor of 2, the numerical fit is not well determined. The third is that the values seem to depend on the method of sample preparation. The average lifetime (Table II, last column) does not depend on the method of preparation.

The polarization anisotropy decay curves shown in Figure 6 have several interesting aspects. We concentrate first on the asymptotic anisotropy which is reached roughly 2 ns after excitation. The values of these asymptotic anisotropies and the corresponding values of the order parameter of the parinaroyl acyl chains according to eq 4a are given in Table IV.[2] The order parameters obtained from these fluorescence measurements may be compared with the values derived from deuterium NMR measurements. In order to make this comparison, we must recall that the parinaroyl polyene chain is rigid so that any internal motions of this labeled chain are restricted to the bonds interconnecting carbon atoms 1–9. As a result, the order parameter obtained from fluorescence should be compared with S_{mol} obtained for C-9 of a flexible, saturated acyl chain where $S_{mol} = -2S_{CD}$ [see, e.g., Seelig & Seelig (1974a)]. This comparison is based on two important assumptions. The first is that the range of motion of the parinaroyl-labeled chains is similar to that of the (deuterium-labeled) saturated acyl chains. The second is that the acyl chain reorientation is complete after roughly 10^{-8} s so that no motion with appreciable amplitude occurs between this time and the deuterium NMR time scale of roughly 10^{-5} s. The comparison of fluorescence and deuterium NMR order parameters shown in Figure 8 indicates that both of these assumptions are valid. The order parameter variation with temperature shows a steep increase near the phase transition temperature, as expected.

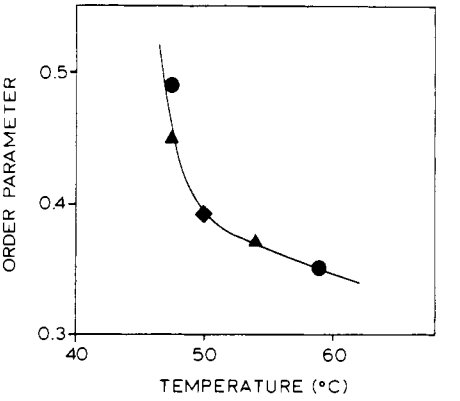

FIGURE 8: Parinaroyl acyl chain order parameters as a function of temperature and comparison with a deuterium NMR order parameter. The solid circles are *trans*-parinaric acid data, the solid triangles are for myristoyl-*trans*-parinaroylphosphatidylcholine (MtPnPC), and the solid diamond is the deuterium NMR result of Seelig & Seelig (1974a).

The value of the order parameter obtained from the asymptotic anisotropy of diphenylhexatriene (DPH) in DPPC at 50 °C is 0.34 (Kawato et al., 1977). This is slightly lower than the (interpolated) parinaric acid value. The difference is fairly small, however, and the DPH experiments are subject to some ambiguity because of uncertainty as to the location of this hydrophobic probe. The relationship between the deuterium NMR and DPH anisotropy order parameter results has recently been discussed by Jähnig (1979) and Heyn (1979).

Another interesting feature of the data of Figure 6 is that the decay of the anisotropy to its asymptotic value is very rapid. Even with the temporal resolution of synchrotron radiation, it is clear that some of the decay is too fast to be detected. This results in a calculated value of the initial anisotropy [r(0)] which is less than 0.4 (Table IV). The observed values of $\langle\phi^{-1}\rangle$ (eq 4b) of 1–2 GHz are therefore probably somewhat low. There is good agreement between the present values of $\langle\phi^{-1}\rangle$ and those for DPH (Kawato et al., 1977, 1978), but this may be due in part to the lack of sufficient resolution in both experiments. Somewhat higher values have been obtained from deuterium NMR T_1 measurements (10 GHz for DPPC at 50 °C; Brown & Seelig, 1979).

The nature of the rapid reorientational motion which gives rise to this anisotropy decay is of considerable interest. There are now numerous indications that the major effect of membrane additives (e.g., cholesterol and proteins) is to decrease the amplitude of this rapid reorientational motion without having much effect on its rate (see below; Wolber, 1980; Kawato et al., 1978, Jähnig, 1979). There are two kinds of acyl chain motion which might reasonably contribute to the

[2] Two values of the asymptotic anisotropy and the corresponding order parameter are given in Table IV, labeled by the subscripts "fit" and "tail". These quantities are defined by eq 5 and the following discussion. Note that the values of S_{tail} are usually greater than those of S_{fit}. This is probably due to a small contribution from the tail of the excitation pulse which increases r and thus S. The fact that two different numerical methods are available for the evaluation of S increases confidence in the values of S_{fit}. The discussion and Figure 8 refer to S_{fit}. There is also an additional experimental test of the anisotropy decay function $r(t)$ due to the fact that the integral of $r(t)$, weighted by the normalized total decay function, should give the steady-state anisotropy (Sklar et al., 1977b; Wolber, 1980).

depolarization of parinaric acid fluorescence. One is the introduction or loss of a gauche bond at any of the single bonds between carbons 1 through 9. This results in a swing of the parinaroyl chromophore through an angle of 60°. According to eq 4a, an elementary excitation of this type would lower the order parameter from its initial value of unity to a value of $^1/_2\,(3\cos^2 60° - 1) = -^1/_8$. Thus, such excitations are very effective at decreasing the order parameter. A second potentially important type of depolarizing motion is the rigid body reorientation of the entire acyl chain. This may involve the off-director wobbling or circulation of the entire phospholipid molecule. The reorientation angle associated with execution of this motion by a single chain is not specified in this model. Its mean-square value, of course, would determine the asymptotic anisotropy.

This type of rigid acyl chain motion was discussed by Petersen & Chan (1977). On the basis of magnetic resonance measurements, they concluded that motions of this type were occurring at a rate of 10^7 to 10^8 s^{-1} with an amplitude of about 50°, corresponding to a change in the order parameter of 0.9. The parinaric acid anisotropy decay of Figure 6 does not show any decay with significant amplitude in the 10^7–10^8-s^{-1} time domain. In particular, the agreement noted above between the value of the order parameter obtained from the anisotropy at $\sim 10^{-8}$ s with the deuterium NMR value indicates that any relaxation which occurs in the 10^{-8}–10^{-5}-s time range does not have an appreciable amplitude ($\Delta S < 0.1$). It is conceivable that the 10^9–10^{10}-s^{-1} orientational relaxation observed for parinaric acid corresponds to a motion which is much slower (10^7–10^8 s^{-1}) for saturated acyl chains which do not have the conjugated polyene tail. This means that the presence of the rigid chromophore must speed up the chain motion by 1–3 orders of magnitude. While this may, at first, seem unreasonable, it could be rationalized by thinking of a parinaroyl chain as a rigid stick at the end of a flexible string (or connected to a pivot). The rigid end of this chain dips into the very mobile interior region of the bilayer where it experiences relatively large amplitude thermal forces. By comparison, a less rigid, saturated acyl chain may resist this driving force by flexing. This ad hoc explanation is intended to emphasize that detailed comparisons of the results of different methods require careful examination of the experimental samples.

Differences between deuterium NMR and spin-label ESR-derived order parameters have been rationalized in terms of an acyl chain motion with a time scale around 10^{-7} s (Gaffney & McConnell, 1974). The basic argument used in this analysis is that angular motions in the 10^7–10^6-s^{-1} frequency range will be averaged over in a deuterium NMR measurement but will appear as a static tilt in an ESR spin-label measurement. Differences between these two experiments may therefore be taken as presumptive evidence for this slow motion. This argument implies that the deuterium NMR order parameter will always be less than the corresponding ESR spin-label order parameter. Again, the fluorescence polarization anisotropy results indicate that all of the acyl chain motion is so fast that it should be complete on the ESR time scale and, therefore, our direct experimental results are in conflict with this interpretation.

At this point, we return to the question of the nature of the fast reorientational motion seen in these fluorescence experiments. It should be remembered that certain types of acyl chain motion will not cause reorientation of the polyene chromophore and therefore depolarization. An example of such a motion is rotation about the long axis of the acyl chain when it is in its all-trans conformation. Another such motion, often mentioned in discussions of NMR relaxation times, is kink diffusion, the concerted rotation process by which a gauche(plus),trans,gauche(minus) sequence diffuses along an acyl chain.

Gauche to trans and trans to gauche isomerizations at bonds 1 through 9 and rigid body motions of the entire chain seem to us to be the most likely candidates for this rapid motion. Rigid body reorientation of a parinaroyl chain containing a gauche bond is, in a sense, an intermediate case with regard to the other two since it requires that the chain have a gauche bond at bonds 1 through 9 but not that gauche–trans excitation be rapid relative to the rigid body rotation. A simple experiment which should distinguish these three reorientational mechanisms is easily devised. Consider the $r(t)$ curves expected for an analogue of parinaric acid with a shorter methylene chain, e.g., two methylenes instead of seven. If rigid body motion not requiring excitation of gauche conformations is the dominant mode of depolarization, then the $r(t)$ curve should be the same as that for parinaric acid. If gauche excitations are required either as the sole mode of depolarization or in conjunction with rigid body motions, then the $r(t)$ curve will be raised at all values of time. This will appear as an increase in the value of the asymptotic anisotropy if rigid body motion of a bent chain is the rapid step and as a decreased rate of approach to the asymptotic anisotropy if gauche bond excitation is the rapid step. The fact that this hypothetical experiment leads to distinct predictions about the anisotropy decay curves demonstrates the unique capability of these types of measurements.

The effect of cholesterol on the motion of parinaroyl chains in bilayers can be discussed in terms of the asymptotic anisotropy (and a corresponding order parameter) and in terms of the relaxation rate, $\langle\phi^{-1}\rangle$. A clear increase in the value of r_∞ with increasing cholesterol content is shown in Figure 7 and Table IV. These results are in good quantitative agreement with those of Kawato et al. (1978). A very similar effect has been observed in a deuterium NMR study of perdeuterated stearic acid in egg phosphatidylcholine at 30 °C. The order parameter for the C-9 position is 0.47, 0.52, 0.60, and 0.78 for 0%, 10%, 20%, and 30% cholesterol (Stockton & Smith, 1976).

The effect of cholesterol on the rate of reorientational motion is probably small. The values of $\langle\phi^{-1}\rangle$ obtained from flashlamp experiments at 53 °C were 0.53, 0.54, 0.22, and 0.078 GHz for 0, 0.1, 0.2, and 0.3 mol fraction of cholesterol (Table IV). This variation in $\langle\phi^{-1}\rangle$ is, however, probably an artifact of the increasing difficulty of the deconvolution problem as the cholesterol content is increased. It is clear from a comparison of the $r(0)$ and $\langle\phi^{-1}\rangle$ values obtained with flashlamp and synchrotron radiation that there is a very rapid component of the anisotropy decay which is too fast to be adequately resolved with flashlamp excitation. This resolution becomes more difficult as the cholesterol content is increased because of the decrease in the amplitude of this fast component. The values of $\langle\phi^{-1}\rangle$ obtained from the synchrotron experiments are 1.9, 2.0, and 6.7 GHz for 59 °C and 0, 0.1, and 0.2 mol fraction of cholesterol. The last number is thought to be higher than the true value based on the unphysical value of $r(0)$ obtained. Our limited data are, on the whole, consistent with the conclusions drawn from DPH anisotropy decay (Kawato et al., 1978) and ^{13}C NMR relaxation studies (Godici & Landsberger, 1975) that cholesterol has, at most, a small effect on the rate of reorientational motion of acyl chains.

The simplest model for the effect of cholesterol on acyl chain motion is one in which acyl chains which are adjacent to the

steroid are completely inhibited from undergoing the rapid depolarizing motion which characterizes the unperturbed bilayer. The anisotropy is then the sum of a time-independent part and an $r(t)$ which is the same as that for pure DPPC. If we assume that the anisotropy for the "immobilized" chains is the same as the 38 °C value of Figure 6, we may calculate the number of chains perturbed per cholesterol. The value obtained is 1.5 chains per cholesterol. A more realistic model would suppose a partial restriction of the angular space allowed the adjacent chains and a correspondingly larger number of perturbed chains.

It seems unlikely that cholesterol would inhibit a rigid body motion of phospholipids which involved the entire molecule or collections of molecules. It does seem to be quite plausible that the rigid steroid ring system would inhibit the introduction of gauche bonds in the upper portion of the acyl chain. This leads us to suggest that the rapid depolarizing motion in fluid bilayers consists of gauche excitations in the upper part of the acyl chains.

Acknowledgments

We wish to acknowledge the assistance of, or helpful discussions with, Sergio Aragon, Ludwig Brand, Michael Brown, Sunney Chan, Craig Cornelius, Frederick Dahlquist, David Kimelman, Charles Klopfenstein, Michael Paddy, Robert Simoni, Larry Sklar, and Amy Tsai. We also wish to thank the Stanford Synchrotron Radiation Laboratory for use of the SLAC facility and Professor Lubert Stryer for permission to use his Ortec single photon counting lifetime apparatus at SLAC. We thank Glenda Dean and Mary Gilland for assistance in the preparation of this manuscript.

References

Andrews, J., & Hudson, B. (1978) *Chem. Phys. Lett. 57*, 600.
Bangham, A. D. (1972) *Chem. Phys. Lipids 8*, 386.
Bauer, D. R., Hudson, B., & Pecora, R. (1975) *J. Chem. Phys. 63*, 588.
Bocian, D. F., & Chan, S. I. (1978) *Annu. Rev. Phys. Chem. 29*, 307.
Brady, G. W., & Fein, O. B. (1977) *Biochim. Biophys. Acta 464*, 249.
Brown, M. F. (1979) *J. Magn. Reson. 35*, 203.
Brown, M. F., & Seelig, J. (1979) *J. Chem. Phys. 70*, 5045.
Carreira, L. A. (1975) *J. Chem. Phys. 62*, 3851.
Chen, L. A., Dale, R. E., Roth, S., & Brand, L. (1977) *J. Biol. Chem. 252*, 2163.
Chen, R. F., & Bowman, R. L. (1965) *Science (Washington, D.C.) 147*, 729.
Davis, J. (1979) *Biophys. J. 27*, 339.
Evans, G. T. (1979) *J. Chem. Phys. 70*, 2362.
Evans, G. T., & Knauss, D. C. (1980) *J. Chem. Phys. 72*, 1504.
Gaber, B. P., & Peticolas, W. L. (1977) *Biochim. Biophys. Acta 465*, 260.
Gaffney, B. J., & McConnell, H. M. (1974) *J. Magn. Reson. 16*, 1.
Gafni, A., Molin, R. L., & Brand L. (1975) *Biophys. J. 15*, 263.
Godici, P. E., & Landsberger, F. R. (1975) *Biochemistry 14*, 3927.
Grinvald, A., & Steinberg, I. Z. (1974) *Anal. Biochem. 59*, 583.
Gupta, C. M., Radhakrishnan, R., & Khorana, H. G. (1977) *Proc. Natl. Acad. Sci. U.S.A. 74*, 4315.
Hemminga, M. A., & Berendson, H. J. C. (1972) *J. Magn. Reson. 8*, 344.
Heyn, M. P. (1979) *FEBS Lett. 108*, 359.
Hubbell, W. L., & McConnell, H. M. (1971) *J. Am. Chem. Soc. 93*, 314.
Isenberg, I. (1975) *Biochemical Fluorescence: Concepts* (Chen, R. F., & Edelhock, H., Eds.) Vol. 1, pp 43–75, Marcel Dekker, New York.
Jähnig, F. (1979) *Proc. Natl. Acad. Sci. U.S.A. 76*, 6361.
Janiak, M. J., Small, D. M., & Shipley, G. G. (1976) *Biochemistry 15*, 4575.
Jost, P., Waggoner, A. S., & Griffith, O. H. (1971) in *Structure and Function of Biological Membranes* (Rothfield, L., Ed.) Academic Press, New York.
Kawato, S., Kinosita, K., Jr., & Ikegami, A. (1977) *Biochemistry 16*, 2319.
Kawato, S., Kinosita, K., Jr., & Ikegami, A. (1978) *Biochemistry 17*, 5026.
Kinosita, K., Jr., Kawato, S., & Ikegami, A. (1977) *Biophys. J. 20*, 289.
Knauss, D. C., & Evans, G. T. (1980) *J. Chem. Phys. 72*, 1499.
Krbecek, R., Gebhardt, C., Gruler, H., & Sackmann, E. (1979) *Biochim. Biophys. Acta 554*, 1.
Kremer, J. M. H., van der Esker, M. W. J., Pathmomanoharam, C., & Wiersema, P. H. (1977) *Biochemistry 16*, 3932.
Lakowicz, J. R., Prendergast, F. G., & Hogen, D. (1979) *Biochemistry 18*, 508.
Lasaga, A. (1976) Thesis, Harvard University, Cambridge, MA.
Leskovar, B., Lo, C. C., Hartig, P. R., & Sauer, K. (1976) *Rev. Sci. Instrum. 47*, 1113.
Luna, E. J., & McConnell, H. M. (1977) *Biochim. Biophys. Acta 466*, 381.
Morgan, C. G., Hudson, B., & Wolber, P. K. (1980) *Proc. Natl. Acad. Sci. U.S.A. 77*, 26.
Munro, I., Pecht, I., & Stryer, L. (1979) *Proc. Natl. Acad. Sci. U.S.A. 76*, 56.
Oldfield, E., Meadows, M., Rice, D., & Jacobs, R. (1978) *Biochemistry 17*, 2727.
Paddy, M. R., Dahlquist, F. W., Davis, J. H., & Bloom, M. (1980) *Biochemistry* (in press).
Petersen, N. O., & Chan, S. I. (1977) *Biochemistry 16*, 2657.
Rand, R. P., Chapman, D., & Larsson, K. (1975) *Biophys. J. 15*, 1117.
Seelig, A., & Seelig, J. (1974a) *Biochemistry 13*, 4839.
Seelig, A., & Seelig, J. (1974b) *Biochem. Biophys. Res. Commun. 51*, 406.
Seiter, C. H. A., & Chan, S. I. (1973) *J. Am. Chem. Soc. 95*, 7541.
Shrager, R. I. (1970) *J. Assoc. Comput. Mach. 17*, 446.
Sklar, L. A. (1976) Ph.D. Thesis, Stanford University, Stanford, CA.
Sklar, L. A., Hudson, B. S., & Simoni, R. D. (1975) *Proc. Natl. Acad. Sci. U.S.A. 72*, 1649.
Sklar, L. A., Hudson, B. S., Petersen, M., & Diamond, J. (1977a) *Biochemistry 16*, 813.
Sklar, L. A., Hudson, B. S., & Simoni, R. D. (1977b) *Biochemistry 16*, 819.
Sklar, L. A., Hudson, B., & Simoni, R. D. (1980) *Methods Enzymol.* (in press).
Smith, B. A., & McConnell, H. M. (1978) *Proc. Natl. Acad. Sci. U.S.A. 75*, 2759.
Stockton, G. W., & Smith, I. C. P. (1976) *Chem. Phys. Lipids 17*, 251.

Tsai, A., Hudson, B., & Simoni, R. D. (1980) *Methods Enzymol.* (in press).
Warshel, A., & Karplus, M. (1972) *J. Am. Chem. Soc. 94*, 5612.
Watts, A., Harlos, K., Maschke, W., & Marsh, D. (1978) *Biochim. Biophys. Acta 510*, 63.
Wolber, P. K. (1980) Ph.D. Thesis, Stanford University, Stanford, CA.
Yellin, M., & Levin, I. W. (1977a) *Biochim. Biophys. Acta 468*, 490.
Yellin, N., & Levin, I. W. (1977b) *Biochim. Biophys. Acta 489*, 177.

Characterization of Pepsin-Resistant Collagen-like Tail Subunit Fragments of 18S and 14S Acetylcholinesterase from *Electrophorus electricus*†

Carol Mays‡ and Terrone L. Rosenberry*

ABSTRACT: Digestion of 18S and 14S acetylcholinesterase from eel electric organ with pepsin at 15 °C for 6 h results in extensive degradation of the catalytic subunits, but a major portion of the collagen-like tail structure associated with these enzyme forms resists degradation. The pepsin-resistant structures partially aggregate and can be isolated by gel exclusion chromatography on Sepharose CL-6B in buffered 1 M sodium chloride. The largest structure, denoted F_3, has a molecular weight of 72000 according to gel electrophoresis in sodium dodecyl sulfate and is composed of three 24000 molecular weight polypeptides linked by intersubunit disulfide bonds. This structure is largely, but not completely, a collagen-like triple helix as indicated by a circular dichroism spectrum typical of triple-helical collagen and an amino acid composition characterized by 27% glycine, 5% hydroxyproline, and 5% hydroxylysine. Continued pepsin action results in degradation of the disulfide linkage region such that disulfide-linked dimers F_2 and finally F_1 monomers become the predominant forms in sodium dodecyl sulfate. Digested samples in which either F_3 or F_2 predominate have virtually identical circular dichroic spectra and amino acid compositions and generate similar diffuse 24000 molecular weight polypeptides following disulfide reduction. Thus the intersubunit disulfide linkages in F_3 must occur close to the end(s) of the fragment polypeptide chains. Pepsin conversion of F_3 to F_2 is particularly accelerated between 25 and 30 °C, suggesting that the triple-helical structure in the disulfide linkage region undergoes thermal destabilization in this temperature range. Digestion at 40 °C yields presumably triple-helical F_1 structures devoid of disulfide linkages, although their degradation to small fragments can be detected at this temperature. The question of whether the three tail subunits that give rise to F_1 polypeptides are identical remains open.

Acetylcholinesterase (EC 3.1.1.7) from the electric organs of the eel *Electrophorus electricus* is extracted at high ionic strength as a mixture of asymmetric forms (Massoulié & Rieger, 1969). The predominant form, an 18S species, can be categorized[1] as an A_{12} molecule and is composed of twelve catalytic subunits (Rieger et al., 1976) linked asymmetrically by disulfide bonds to three collagen-like tail subunit polypeptides (Rosenberry & Richardson, 1977; Anglister & Silman, 1978; Rosenberry et al., 1980). A similar tail structure has been identified in the 14S (A_8) and 8S (A_4) forms that are also present in these extracts (McCann & Rosenberry, 1977). The A_{12} nature of the principal asymmetric form from several rat, chicken, and human muscles and from bovine superior cervical ganglion also has been confirmed (Bon et al., 1979), but, in contrast to eel electric organ, these tissues also contain considerable amounts of globular G_4, G_2, and G_1 forms (Massoulié, 1980). The A_{12} form in rat diaphragm is localized primarily in the end-plate region and virtually disappears on denervation of the muscle (Hall, 1973), while the globular forms are distributed nearly uniformly in this muscle and show a much smaller decrease on denervation. A basement membrane localization of a significant fraction of end-plate acetylcholinesterase by means of its collagen-like tail was suggested by observations that collagenase degrades end-plate basement membrane and releases this enzyme from the end plate (Hall & Kelly, 1971; Betz & Sakmann, 1973), and this suggestion was supported by direct observation of acetylcholinesterase activity in the end-plate basement membrane matrix that survived selective destruction of nerve and muscle cell elements (McMahan et al., 1978). Although end-plate A_{12} forms have not been isolated and subjected to subunit analysis, the similarities of end-plate and electric organ A_{12} forms in their native molecular weights (Bon et al., 1979) and their solubility, aggregation, and collagenase digestion patterns (Bon et al., 1978, 1979; Johnson et al., 1977; Watkins et al., 1977; Webb, 1978; Anglister & Silman, 1978; Rotundo & Fambrough, 1979) indicate that their collagen-like tail structures must be quite comparable.

† From the Departments of Biochemistry and Neurology, College of Physicians and Surgeons, Columbia University, New York, New York 10032. *Received August 21, 1980; revised manuscript received January 6, 1981.* This investigation was supported, in part, by National Institutes of Health Grants NS-03304 and NS-11766, by National Science Foundation Grant PCM77-09383, by the Muscular Dystrophy Association, and by the New York Heart Association.

* Correspondence should be addressed to this author at the Department of Pharmacology, Case Western Reserve University, Cleveland, OH 44106.

‡ Present address: The Division of Arteriosclerosis and Metabolism, Mount Sinai School of Medicine, New York, NY 10029.

[1] This nomenclature (Bon et al., 1979) distinguishes two classes of acetylcholinesterase: "asymmetric" forms A_n that are assemblies of n catalytic subunits associated with a collagen-like tail structure and "globular" forms G_n in which the assemblies of n catalytic subunits are devoid of a collagen-like tail.

0006-2960/81/0420-2810$01.25/0